Fatigue strength of tensile plates with combined attachments

Zhi-Gang Xiao*, Kentaro Yamada**

*M. of Eng., Dept. of Civil Eng., Nagoya University, Furocho, Chikusa-ku, Nagoya 464-8603
**Ph.D., Professor, Department of Environmental Engineering and Architecture, Graduate School of Environmental Studies, Nagoya University, Furocho, Chikusa-ku, Nagoya 464-8603

Fatigue tests were carried out on tensile plates with combined welded attachments. It is found that fatigue strength is affected by combination form of attachments, attachment length, and presence of scallop, which is confirmed by 3D finite element analyses (FEA). The one-millimeter approach was also used to evaluate fatigue strength of tensile plates with combined attachments. The valuation was in good agreement with fatigue test results. Fatigue test data and FEA results of combined attachments were also compared with those of single attachments. Referring to experimental results, evaluations by one-millimeter approach, and fatigue strength of single attachments suggested by fatigue design recommendations, fatigue strengths were proposed for combined attachments.

Key Words: fatigue test, combined attachments, one-millimeter approach, FEA (finite element analysis)

1. Introduction

Combination of welded attachments is often seen in welded steel structures. The combined use of attachments may result in intersection of two, three or more welds. Since it is difficult to guarantee the quality of weld at intersecting region, scallops are sometimes introduced to avoid weld intersection.

Fatigue strength of single attachment, such as longitudinal or transverse attachments, can be obtained by referring to fatigue design codes or recommendations. In Table 1, fatigue strengths of as-welded transverse and longitudinal attachments suggested by Japanese Society of Steel Construction (JSSC)[1] and International Institute of Welding (IIW)[2] are listed. Very few fatigue tests on combined attachments have been carried out and the fatigue behaviors of combined attachments are still not clarified. In this study, fatigue tests were carried out on seven sets of tensile plates with combined attachments. Fatigue strengths of the tensile plates were evaluated with one-millimeter approach based on FEM analyses. Good agreement between evaluations and fatigue test results was achieved. Fatigue behaviors of combined attachments were also compared with those of single attachments. Based on predictions and fatigue test results, fatigue strengths were recommended for combined attachments.

2. Fatigue Tests

2.1 Test specimens

Two types of fatigue test specimens are designed with attachments intersecting at right angles. In one type, a longitudinal attachment intersects with a transverse attachment at the middle of the transverse one, as shown in Fig.1a. For simplicity, the longitudinal attachment is hereinafter referred to as gusset, and the transverse attachment as transverse stiffener or stiffener. The lengths of gussets are 50, 100 and 200 millimeters. They are named as T-type specimens. In the other type of specimens, the gusset intersects at both ends with two transverse stiffeners, as shown in Fig.1b. They are named as H-type specimens.

For both types, the intersecting attachments are symmetrically fillet-welded to both surfaces of the base plate. The fillet welds between attachments and those between attachment and base plate are of equal leg length of 6 mm. Some specimens are also designed with scallop of 35 mm in radius to avoid intersection of fillet welds. T-type specimens are subdivided into TN- (without scallop) and TS-specimens (with scallop), and H-type into HN200 and HS200. The steel plates used for manufacturing the specimens confirmed to steel SM490YA of Japanese Industrial Standard JIS G3106[3]. Mechanical properties and chemical compositions of the plates are listed in Table 2.

Table 1 Fatigue strength of as-welded single attachment

	Non-load-carrying cruciform joint	Out-of-plane gusset
JSSC	JSSC-E (80MPa at 2 million cycles)	JSSC-F (65MPa), when $l^{*} \geq 100$ mm JSSC-G (50MPa), when $l<100$mm
IIW	FAT 80 (80MPa at 2 million cycles)	FAT 80, when $l<50$ mm FAT 71, when $l<150$ mm FAT 63, when $l<300$ mm FAT 50, when $l>300$ mm

Note: * l is the length of the longitudinal attachment.

Table 2 Mechanical properties and chemical compositions of steel

Yield strength (MPa)	Ultimate tensile strength (MPa)	Elongation (%)	Chemical compositions (%)				
			C	Si	M	P	S
440	550	22	0.17	0.19	1.37	0.015	0.004

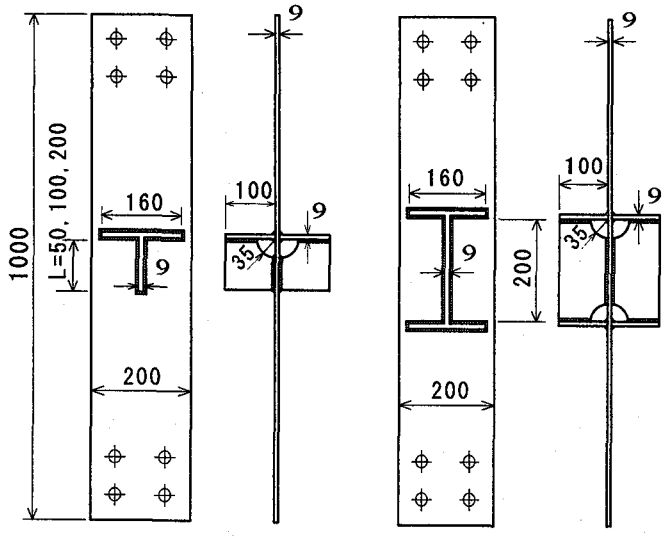

(a) TN and TS type b) HN and HS type

Fig.1 Fatigue test specimens

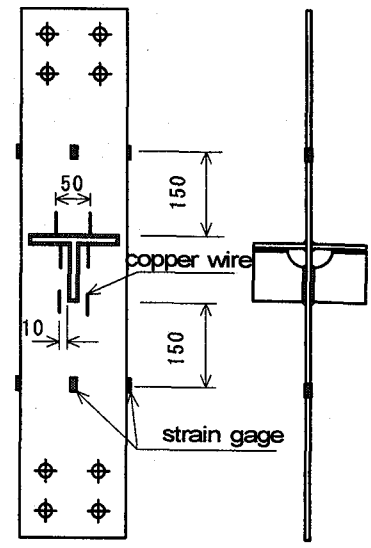

Fig.2 Location of copper wires and strain gages

2.2 Fatigue tests

Constant amplitude fatigue tests were carried out with an Amsler type fatigue-testing machine with the loading capacity of 980kN. The minimum tensile stress was set at 27MPa through all tests. Cyclic loading was applied at the rate of 270 cycles per minute. Eight strain gages were attached to the surfaces and edges of the tensile plate to check the alignment of it with the jigs of the testing machine, and one of them was used to monitor loading during fatigue test. Copper wires of 0.04mm in diameter were adhered to the surfaces of test specimen to define fatigue life. These wires were connected into the load controlling circuit of the testing machine to stop the machine automatically when fatigue cracks cutting the wire. The number of loading cycles when fatigue crack cut the wire is defined as final fatigue life in this study. Fig.2 shows schematically the locations of strain gage and copper wire.

Dye marking test and beach marking test were also carried out. Dye marking left visible fatigue cracks on the fracture surface. Beach marking test traced progress of fatigue crack by changing the applied stress range into half.

2.3 Fatigue test results

Crack initiation and propagation. Fig.3 shows the location of fatigue cracks. In TN- and TS-specimens, the fatigue cracks were initiated and propagated at the weld toe of the short transverse fillet weld around the 'free' end (the end not welded to transverse stiffener) of gusset. The fatigue cracks of HN200 formed at fillet weld toe of transverse stiffener at the outside fillet weld. The fatigue cracks in HS200 developed at the toe of the ending weld at scallop

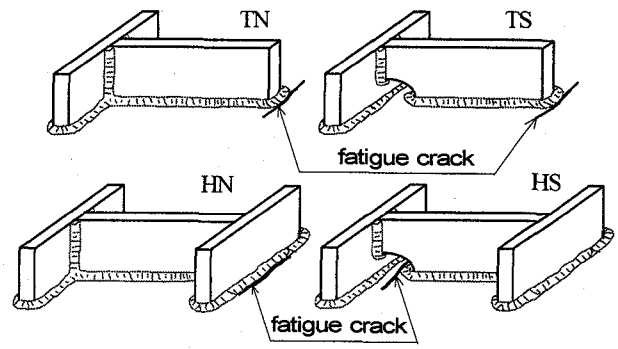

Fig.3 Location of fatigue cracks

edge.

Some typical fracture surfaces are shown in Fig.4. In all specimens the cracks were initiated at several points along weld toe, and these semi-elliptical cracks propagated into the thickness direction of the tensile plate. Then they coalesced into a large flat semi-elliptical crack, which continued its propagation, penetrated the thickness of the tensile plate, and cut the copper wire. The length of crack on plate surface is about 50 mm when copper wire is cut.

Fatigue test results. Fatigue test results of all specimens are listed in Table 3, and plotted in Fig.5. If giving fatigue strength in terms of lower bound of test data in the limited life region, the fatigue class JSSC-F may be assigned to all types of specimens except TN50, for which JSSC-E may be suggested. The regression S-N lines for each set of specimens are also solved with the inverse of the slope being set at m=3, as shown in Eq. 1.

Table 3 Fatigue life of test specimens (in kilocycles)

Specimen	Stress range			
	82MPa	105MPa	122MPa	140MPa
TN50		1243	1124 760	523 450
TN100	>4771*	989*	705 841	309 284
TN200	1589 2134	739	573 549	
TS100		1111 895	791 603	364
TS200	1488 1018	989	440 438	
HN200	>7940*	1988* 2131	658 684	434 376
HS200		1153 1581	825 740	417 448

Note: * Specimens retested at 105 MPa after 4771 and 7940 kilocycles at 82MPa without cracks being found

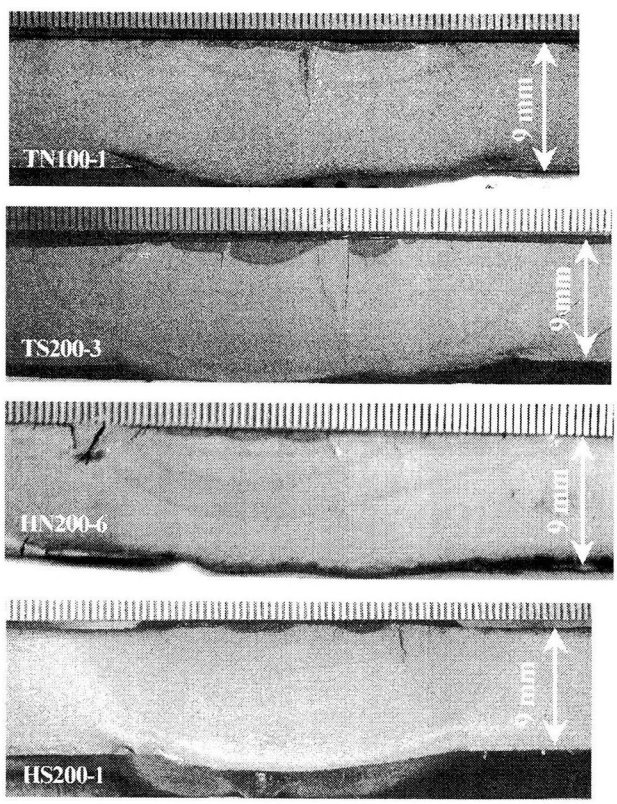

Fig.4 Fracture surfaces

$$\log N = c - 3 \times \log S_r \quad (1)$$

where, N is the number of cycles of stress range to failure, and S_r is the stress range in MPa. Results of regression analyses for test results are listed in Table 4. The standard deviation s is calculated by taking $\log N$ as dependent variable, and the mean fatigue strength is the stress range at 2 million cycles to failure obtained from regression analysis. The runout data are not included in the analysis.

Table 4 Regression analyses of test results

Specimen	c	s	Mean strength at 2 million cycles (MPa)
TN50	12.17	0.083	90.5
TN100	12.03	0.123	81.4
TN200	11.99	0.056	78.7
TS100	12.06	0.067	83.3
TS200	11.90	0.111	73.6
HN200	12.16	0.140	89.6
HS200	12.16	0.080	89.5

The mean strength values shown in Table 4 demonstrate that fatigue strengths of TN- and TS-specimens decrease with the increase of gusset length. Since in these specimens, cracks form at gusset end, where stress concentration increases with gusset length. Comparison of TN- with TS-specimens results in conflicting results. Mean strength of TS-100 is slightly larger than that of TN-100 while TS-200 is evidently less than TN-200. The contradiction may be due to the limited number of test data. Only five data are available for each set of specimens.

HN200 and HS200 have very close mean strengths, though fatigue cracks in them develop at different locations. Compared with TN200 and TS200, both of which have the same length of gusset as HN200 and HS200, the fatigue strength of HN200 and HS200 is significantly increased.

3. Finite Element Analyses

3.1 FEA model

Fatigue cracks in all specimens developed at the weld toe where existed high stress concentration. FEA was carried out for each type of specimen to comprehend test results. FEA results were also used in the evaluation of fatigue strength by one-millimeter approach.

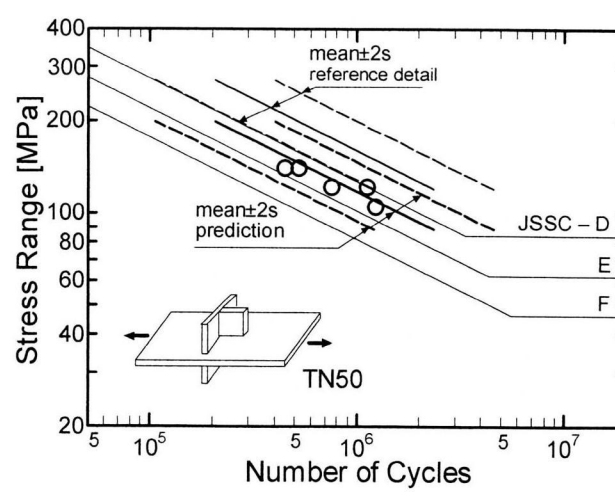

(a) TN50

Fig.5 Fatigue test results and evaluations (to be continued)

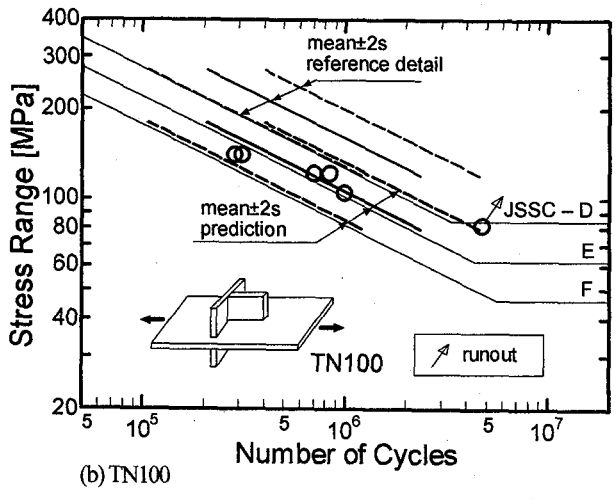

(b) TN100

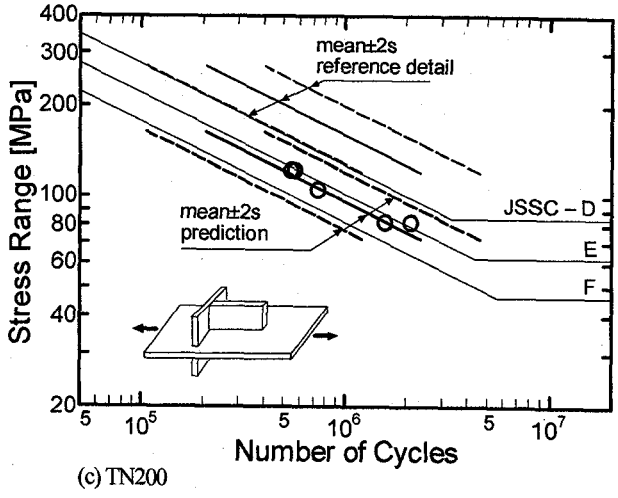

(c) TN200

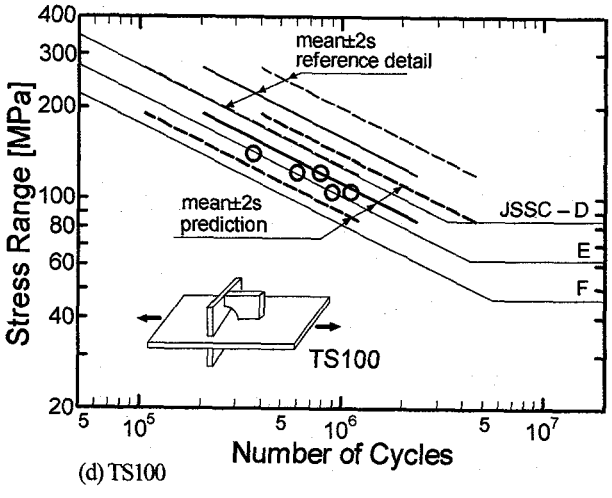

(d) TS100

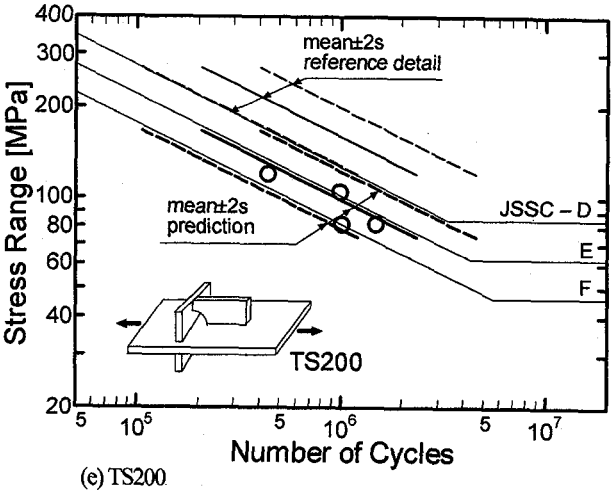

(e) TS200

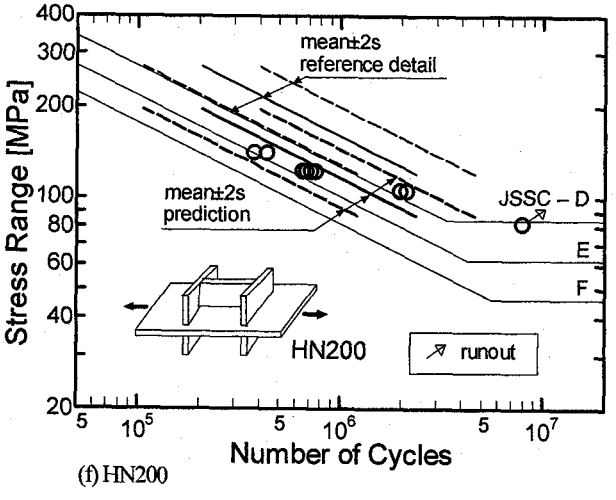

(f) HN200

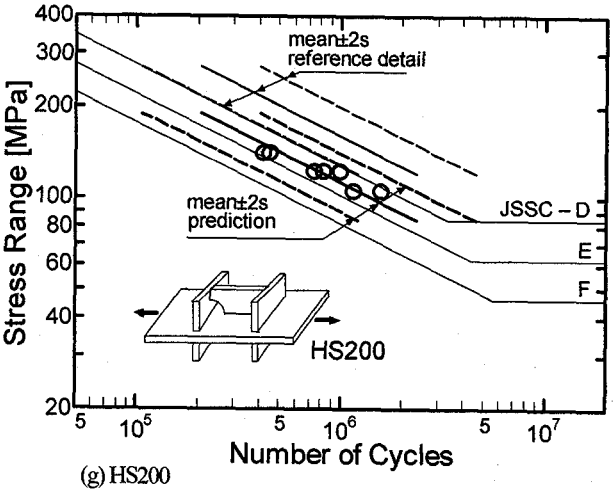

(g) HS200

Fig.5 Fatigue test results and evaluations (continued)

Three-dimensional models of eight-node solid element were created for all types of specimen using the software package Cosmos/M 2.6[4]. The minimum mesh of size 1x1x1 mm was used around regions where high stress concentration was expected. As an example, Fig.6 shows the FEA model of TN100, for which only one quarter of specimen is modeled by taking advantage of symmetry. The fillet weld was modeled with 6 layers of elements, each 1mm thick, with weld toe angle ideally taken as 45 degrees and weld toe radius as zero. The half-thick tensile plate in the model was modeled with 5 layers of elements.

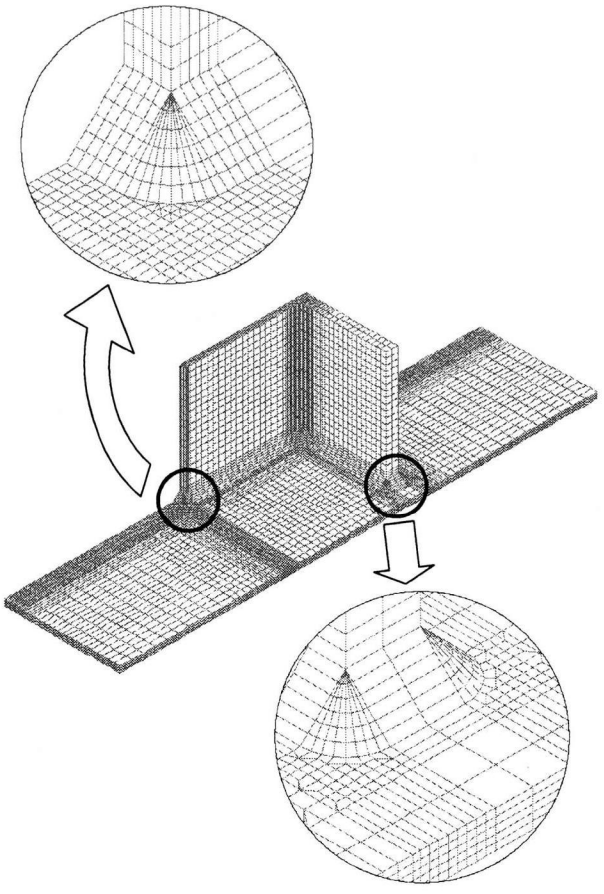

Fig.6 Example of FEM model (TN100)

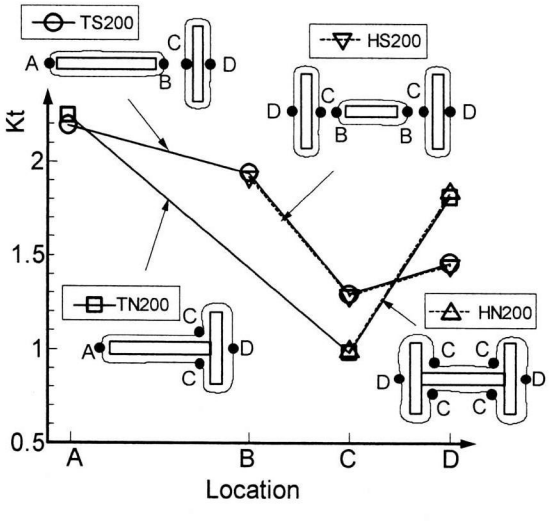

Fig.7 Locations of high stress concentration

3.2. Locations of high stress concentration

For TS-specimens, four locations of highest stress concentration might be listed, as plotted in the inset of Fig.7, i.e. free end of gusset, Point A; the other end of the gusset at scallop edge, Point B; midpoints of transverse stiffener edge at scallop side and the opposite side, Point C and D. For TN-specimens three sites are located, as shown in the inset of Fig.7, free end of gusset, Point A; intersecting point of welds at corner, Pint C and the midpoint of the 'free' side (the side not welded to gusset) of the transverse stiffener, Point D. In HS200 and HN200, the gusset does not have a free end, and other possible locations of highest stress concentration are similar with TS-specimen and TN-specimen, respectively.

In TN- and TS-specimens, the highest stress concentration exists at the free end of gusset, Point A. In HN200, the free edge of the transverse stiffener has the highest stress concentration at its midpoint, Point D. In HS200, the highest stress concentration is at scallop edge. In all specimens tested, fatigue cracks were indeed initiated at locations of the highest stress concentration.

3.3 Stress concentration at free end of gusset

Fig.8 shows the stress distribution near the free end of gusset in TN- and TS-specimens. It can be easily seen from Fig.8 that stress concentration at the free end of gusset in TN- and TS-specimens increases with gusset length. This confirms the trend that fatigue strength of TN- and TS-specimens decreases with gusset length. The presence of scallop in TS-specimens makes the intersecting region of attachments less stiffened, thus leads to a reduced stress concentration at the free end of gusset, comparing with the stress

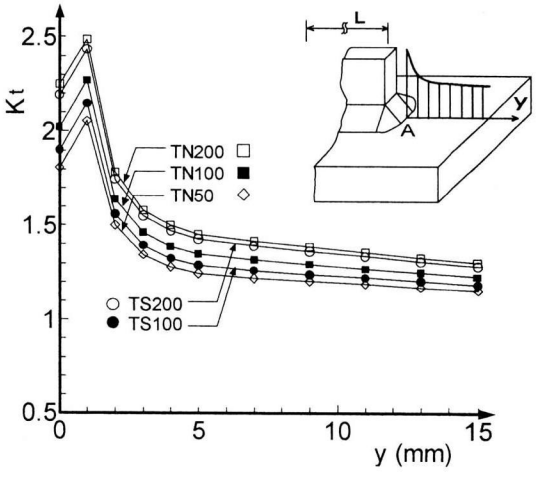

(a) along longitudinal direction

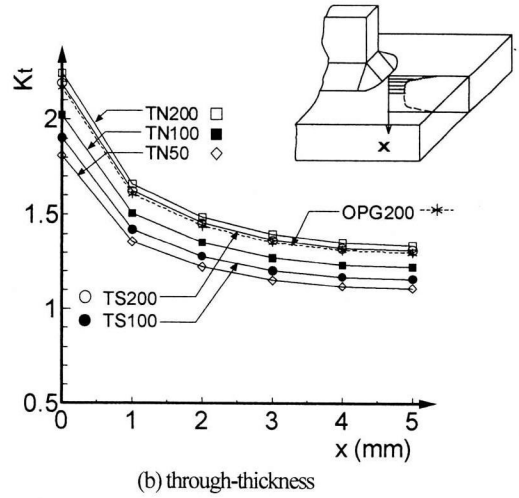

(b) through-thickness

Fig.8 Stress concentration at gusset end

concentration of the TN-specimen with the same length of gusset. The effect of scallop on stress concentration at free end of gusset becomes less significant when gusset becomes longer. This conclusion can be easily drawn by comparing the stress difference between TN100 and TS100 with that between TN200 and TS200, as shown in Fig.8. But the scallop effect is not consistently confirmed by test data. As noted before, probably due to limited number of data, TN200 showed longer life than TS200.

The stress concentration at free end of gusset in T-type specimens is still more severe than that of out-of-plane gusset specimens of the same gusset length due to the stiffening effect of the transverse stiffener, this being concluded by comparison of through-thickness stress distribution of TN200, TS200 and 200 mm long out-of-plane gusset, OPG200, Fig.8b. Except not having transverse stiffener, other components in OPG200 are of the same dimension as those in TN200.

One point to note here is that, in Fig.8a, the stress concentration at the first node (y=0) is less than that at the second node. This phenomenon is also shown in Fig.9. The reason behind is that the nodal stress presented here is the averaged value among elements sharing the common node. The nodal stresses of elements at the weld side are relatively small and thus averaging stress makes stress value at the first node smaller.

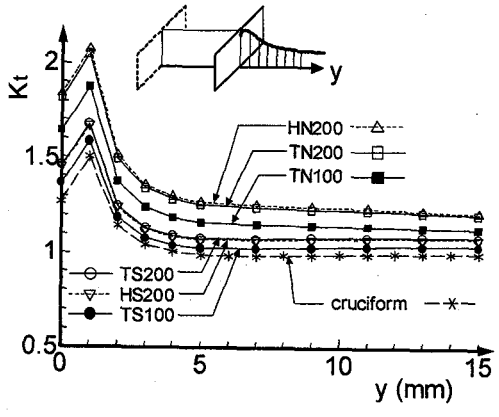

Fig.9 Stress concentration at stiffener edge

3.4 Stress concentration at free edge of stiffener

The length of gusset also demonstrates its effect on stress concentration at midpoint of free edge of transverse stiffener, which is shown by the stress distributions of TN- and TS-specimens in Fig.9. It is seen by the comparison of stress distribution of TN200 with HN200, and TS200 with HS200, that the stress concentration at free edge of transverse stiffener is less affected by the presence of transverse stiffener at far end of gusset. However, the scallop has significant effect on stress concentration at free edge of transverse stiffener. The effect of 'separating' the gusset from the transverse stiffener by introducing the scallop makes the stress concentration at Point D (see the inset of Fig.7) in TS200 less than that of TN100 at corresponding point. This means that the effect of scallop outweighs that of gusset length as far as the stress concentration at free edge of transverse stiffener is concerned.

4. Fatigue Strength Evaluation by One-Millimeter Approach

As shown above, fatigue strengths of combined attachments can be comprehended qualitatively by FEA. However, quantitative evaluation without experimenting is more preferable in practice. Focusing on the stress distribution along the expected path of fatigue crack, the authors proposed an approach to evaluating fatigue strength of fillet welded details[5]. It is found by FEM analyses that, along the direction of crack propagation, the local effect of weld profile is limited within 1 mm from crack origin (weld toe). The stress at this location (1 mm in depth, in most cases) is taken as an indicator of global geometry of welded joint and used as a measure of fatigue strength.

The S-N curve to be used with stresses at 1 mm in depth was determined with test data of non-load-carrying fillet welded cruciform joints[6][7], as shown in Fig.10. In the cruciform joints selected, the base plate and attachments are about 10 mm thick and fillets are 6 mm in size, and FEA shows that their stress concentration at 1 mm in depth in weld toe section is close to unity. In these specimens, the main contribution to stress concentration at weld toe region comes from weld profile, and the scatter of test data of these cruciform joints (hereinafter referred to as reference details) is primarily due to variation of weld profile. The applicability of one-millimeter approach was verified by fatigue test results of several types of normal details, such as in-plane gussets and out-of-plane gussets[5].

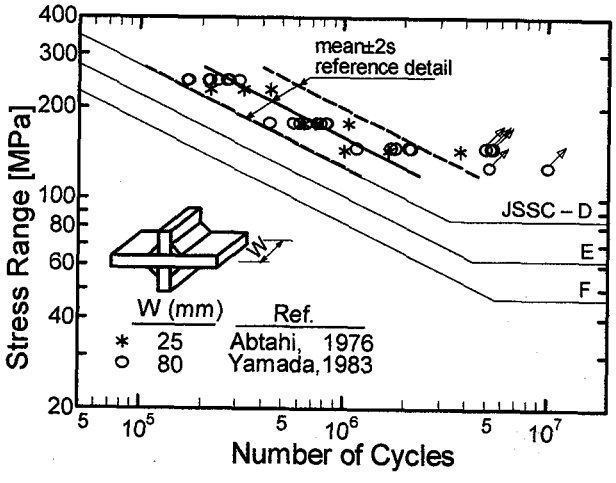

Fig.10 Fatigue test data of reference detail

In this study, the one-millimeter approach is also used to evaluate fatigue strength of combined attachments. Stress at 1mm in depth is extracted for each type of specimens from through-thickness stress distribution as shown in Fig.8b. With the stress at 1mm in depth and the regression S-N curves of the reference detail, fatigue evaluation is carried out for each type of specimen and the result is plotted in Fig.5 along with fatigue test data.

All test data have fallen into the prediction range, which shows that one-millimeter approach is suitable for predicting fatigue life of combined attachments. If giving fatigue strength in terms of the mean-2s prediction without consideration on fatigue limit, JSSC-G

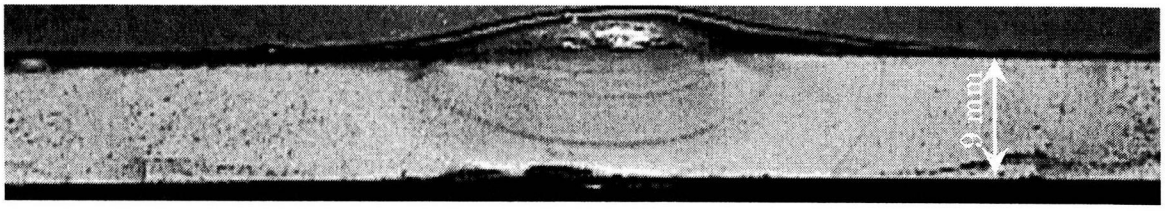

(a) 200 mm long out-of-plane gusset

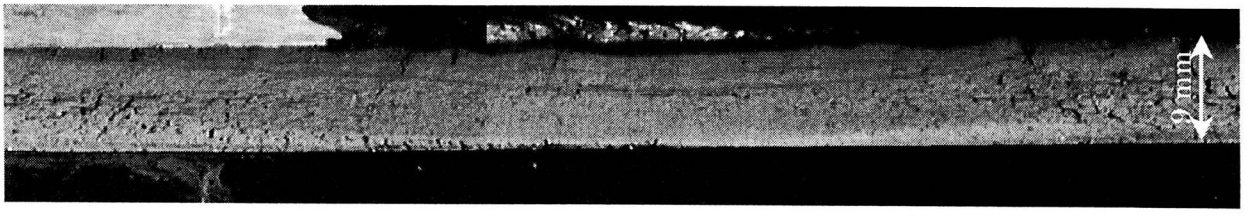

(b) non-load-carrying cruciform joint

Fig.11 Fracture surfaces of single attachment

will be assigned to TN200 and TS200, while JSSC-F to the other types of specimen. The results are the same as strength evaluation given by hot spot stress (HSS) methods except TS200, for which HSS gives the strength of JSSC-F. The HSS evaluations are carried out according to the suggestions provided by IIW[2], Huther[8], and Machida[9], all of which give rather consistent evaluations.

5. Comparison with single attachment

5.1 Comparison of TN- and TS-specimens with out-of-plane gussets

The primary difference of TN- and TS-specimens from out-of-plane gussets is the addition of the transverse stiffener at the end of gusset. Fatigue cracks in all these specimens develop at the end of gusset, where there exists the highest stress concentration. As noted earlier, the stiffening effect of transverse stiffener increases stress concentration at the free end of gusset. However, the increase becomes less significant when gusset becomes longer.

The initiation and propagation of fatigue cracks in TN- and TS-specimens are much similar to out-of-plane gusset. A fracture surface of 200 mm long out-of-plane gusset experimented by Yamada[10] is shown in Fig.11a. Comparison of Fig.11a with crack surfaces of TN- and TS-specimens in Fig.4 shows many similarities in crack initiation and propagation. In all these specimens, multiple cracks developed at weld toe around gusset end. These cracks propagated into the thickness of the tensile plate, coalesced into a large semi-elliptical crack, and finally penetrated the tensile plate.

Fatigue test data of 200 mm long out-of-plane gusset[10] are also plotted against those of TN200 and TS200 in Fig.12. Most of data points are distributed between JSSC-E and F, and no significant difference exists between test data of different specimens. Fatigue strength of TN- and TS-specimens should be assigned at least equal to that of out-of-plane gusset if not less, since the stress concentration at gusset end is slightly larger than that of out-of-plane gusset.

5.2 Comparison of HN200 with out-of-plane gussets and non-load-carrying cruciform joints

Compared with out-of-plane gusset, the addition of transverse stiffeners at both ends of gusset in HN200 spreads the geometric discontinuity over the whole width of base plate, thus alleviates considerably the local stress concentration at gusset end. However, due to the presence of gusset, the stress concentration at the middle of free edge of stiffener in HN200 is still much larger than that of cruciform joints, CRU200 (Fig.9). In CRU200, the main plate is 200mm wide, and the thicknesses of main plate and transverse stiffener are the same as those in HN200. Leg length of fillet weld is also 6mm.

Observation shows that fracture surface of HN200 is more similar to out-of-plane gusset than to cruciform joint. The fracture surface of Fig.11b is taken from a non-load-carrying cruciform joint experimented by Yamada[11]. It shows that many cracks were initiated at weld toe across the large portion of the plate width. After some propagation, these cracks coalesced into a very flat large crack, which is much different from the semi-elliptical cracks of HN200 and out-of-plane gusset.

Fatigue test results of HN200, non-load-carrying cruciform joints[11] and 200 mm long out-of-plane gussets[10] are plotted in

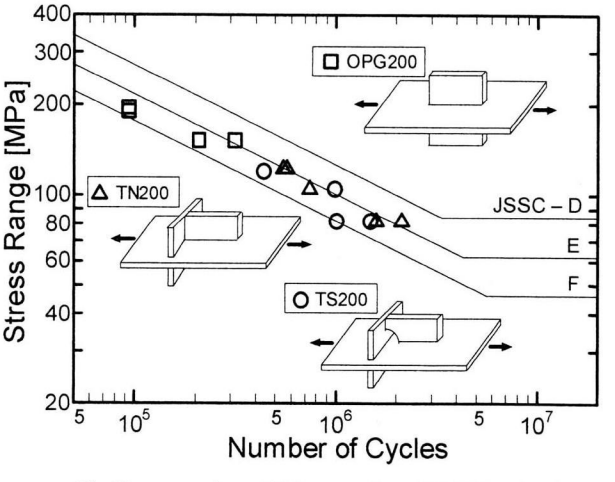

Fig.12 comparison of fatigue test data of TN200 and TS200 with out-of-plane gusset

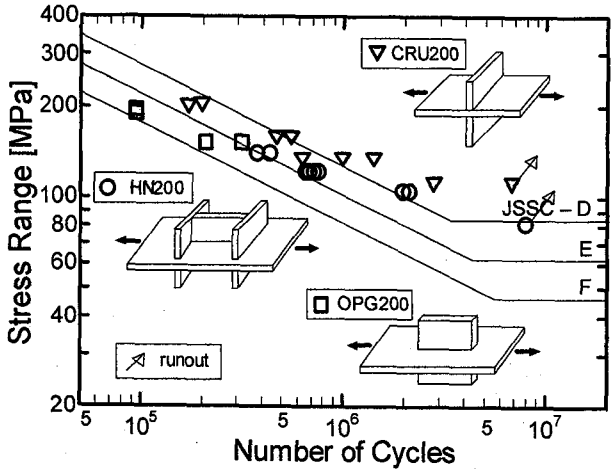

Fig.13 comparison of fatigue test data of HN200 with cruciform joint and out-of-plane gusset

Fig.13 for comparison. Among them, test data of non-load-carrying cruciform joints are distributed in the top region, those of out-of-plane gusset in the bottom, and data of HN200 in between. The reason behind this kind of data distribution is the severity of stress concentration as compared earlier. The fatigue strength suggested by JSSC[1] for as-welded non-load-carrying cruciform joints and out-of-plane gusset (when gusset is longer than 100 mm) is JSSC-E and G, respectively. Thus the evaluation of JSSC-F for HN200 given by one-millimeter approach seems reasonable.

One point to note is that fatigue strength of CRU200 in Fig.13 is lower than that of reference details in Fig.10. Size effect is the main factor accounting for the strength difference. The dimension of reference details was limited within a small range to exclude size effect.

6. Summary

In this study, fatigue behaviors of fillet welded combined attachments are investigated with experiments and finite element analyses. Fatigue evaluations were given in terms of one-millimeter approach. The evaluations are in good agreement with the experimental results.

In T-type specimens, fatigue cracks are initiated at free end of gusset, where exists the highest stress concentration. Stress concentration at gusset end and fatigue strength is sensitive to gusset length. Scallop does not have significant effect on fatigue strength. TN200 and TS200 specimens show similar fatigue strength with out-of-plane gussets OPG200.

In HN200 fatigue cracks form at the central part of the free edge of transverse stiffener, where stress concentration is reduced by the existence of the transverse stiffener if compared with out-of-plane gusset, but still more severe than non-load-carrying cruciform joints due to the presence of the stiffening gusset. The fatigue strengths of HN-specimens are in between those of out-of-plane gusset and non-load-carrying cruciform joints.

In comparison with HN200, cutting scallops in HS200 results in shift of crack location from transverse stiffener edge to scallop edge, without significant change in fatigue strength.

Single transverse attachments (equivalent to non-load-carrying cruciform joint) are the most preferable while the use of longitudinal ones (out-of-plane gussets) should be avoided. Adding a transverse stiffener at one end of gusset cannot increase fatigue strength since fatigue cracks will form at the 'exposed' end. If the use of gusset cannot be avoided, welding transverse stiffeners at both ends will improve fatigue strength considerably.

Acknowledgement

This research was partially supported by the Ministry of Education, Science, Sports and Culture, Grant-in-Aid for Scientific Research (B), 14350241, 2002 and Nagoya Expressway Public Cooperation. The writers also wish to thank Mr. M. Gotoh and Mr. S. Kinoshita for their dedication to the experiments.

References

1) JSSC (Japanese Society of Steel Construction), *Fatige Design Recommendations for Steel Structures [English Version]*, 1995.

2) Hobbacher, A., *Recommendations on Fatigue of Welded Components*, IIW document XIII-1539-96/XV-845-96, 1996.

3) JIS (Japanese Industrial Standard), *Rolled steels for welded structure*, JIS G 3106: 1999. Revised 1999-01-20. Published by Japanese Standards Association.

4) SRAC (Structural Research and Analysis Corp.), *Cosmos/M User's Guide*, Cosmos/M 2.6 online help documents, 2000.

5) Yamada, K., Xiao, Z. G., Kim, I. T., and Tateishi, K., Re-analysis of fatigue test data of attachments based on stress at fillet weld toe, *J. of Struct. Engrg*, JSCE, Vol.48(A), pp.1047-1054, 2002. (In Japanese)

6) Abtahi, A., Albrecht, P., and Irwin, G. R., Fatigue of periodically overloaded stiffener detail, *Journal of the Structural Division, Proceedings of ASCE*, Vol.102, No.ST11, pp.2103-2119, 1976.

7) Yamada, K., Murayama, M., Kondo, A., and Kikuchi, Y., Fatiuge strength of two- and four-year weathered weldments of weathering steels and structural steel. *Proceedings of the Japan Society of Civil Engineers*, No.337, pp.67-74, 1983. (In Japanese)

8) Huther, M., and Henry, J., Recommendation for hot-spot stress definition in welded joints, IIW-IIS document IIW-IIS doc XIII 1416-91.

9) Machida S., Matoba, M., Yoshinari, H., and Nishimura, R., Definition of hot spot stress in welded plate type structure for fatigue assessment, IIW document IIW-XIII-1414-91.

10) Yamada, K., Kato, S., Okabe, A., Kim, I.T., and Ojio, T., Fatigue test of tensile plate with out-of-plane gussets inclined to applied stress, *J. of Struct. Engrg*, JSCE, Vol.47(A), pp.1039-1045, 2001. (In Japanese)

11) Yamada, K., Kim, I.T., and Ito, K., Fatigue behavior of inclined non-load-carrying fillet welded joints, *Journal of Structural Mechanics and Earthquake Engineering*, JSCE, No.682/I-56, pp.383-390, 2001. (In Japanese)

(Received September 13,2002)